Available online at www.sciencedirect.com
ScienceDirect
Earth and Planetary Science Letters 256 (2007) 521–533
EPSL
www.elsevier.com/locate/epsl

Magnesium isotopic constraints on the origin of CB_b chondrites

Matthieu Gounelle [a,b,*], Edward D. Young [c,d], Anat Shahar [d], Eric Tonui [d], Anton Kearsley [b]

[a] *Laboratoire d'Étude de la Matière Extraterrestre (LEME), Muséum National d'Histoire Naturelle, CP52, 57 rue Cuvier, 75005 Paris, France*
[b] *Impacts and Astromaterials Research Center (IARC), Department of Mineralogy, Natural History Museum, Cromwell Road, SW7 5BD London, UK*
[c] *Institute of Geophysics and Planetary Physics, University of California – Los Angeles, Los Angeles, CA90095, USA*
[d] *Department of Earth and Space Sciences, University of California – Los Angeles, Los Angeles, CA90095, USA*

Received 30 August 2006; received in revised form 31 January 2007; accepted 2 February 2007
Available online 11 February 2007
Editor: R.W. Carlson

Abstract

The magnesium isotopic composition of Calcium-, Aluminium-rich Inclusions (CAIs) and chondrules from the CB_b chondrites HH237 and QUE94411 was measured using MC-ICPMS coupled with a laser ablation system.

CAIs from CB_b chondrites exhibit limited mass-dependent fractionation ($\delta^{25}Mg'$ (DSM3) $<1.3‰$) and formed with undetectable ^{26}Al ($^{26}Al/^{27}Al < 4.6\times10^{-6}$). Petrographic observations suggest that CB_b CAIs are igneous. The magnesium isotopic composition of CB_b igneous CAIs contrast with that of CV3 igneous CAIs which are usually mass fractionated and formed with an elevated initial abundance of ^{26}Al. We contend that the absence of ^{26}Al in CAIs is due either to a late formation in the case of a stellar origin of ^{26}Al, or to a lack of exposure to impulsive flares in the case of an irradiation origin of ^{26}Al. In both cases, it implies that a protoplanetary disk was present ~4563 Ma ago, when CB_b chondrites agglomerated.

Chondrules have $\delta^{25}Mg'$ (DSM3) varying from −0.80 to 0.95‰. A rough negative correlation is observed between the $\delta^{25}Mg'$ of chondrules and their $^{24}Mg/^{27}Al$ ratio. This correlation is attributed to evaporation rather than mixing. Contrary to CAIs, chondrules from CB_b chondrites have a magnesium isotopic composition similar to that of CV3 chondrules. This last result is surprising as CB_b chondrules are significantly different from CV3 chondrules in mineralogy and chemistry.

If chondrules from CB_b chondrites formed in an impact-related vapour plume as proposed by Krot et al. [A.N. Krot, Y. Amelin, P. Cassen and A. Meibom, Young chondrules in CB chondrites formed by a giant impact in the early Solar System, Nature 436 (2005) 989–992], our data show that physical conditions in the vapour plume were similar to those of the solar accretion disk at the time and location of the formation of CV chondrules. We note that the oxygen isotopic composition of CAIs is incompatible with their remelting in the putative impact vapour plume. Alternatively, it is possible that CB_b chondrules formed in a protoplanetary disk as the differences between these and "normal" CV3 chondrules can also be explained in term of spatial and temporal variations of the protoplanetary disk. We show that their young Pb–Pb age is not an argument in favour of an impact origin as protoplanetary disks can last as long as 10 Myr around protostars. If CB_b chondrites formed in the solar accretion disk, we speculate they might be the last formed chondrite group. Such a hypothesis might shed light on the unique properties of CB_b chondrites.

Keywords: chondrites; protoplanetary disks; magnesium isotopes; aluminium-26; large impacts; bencubbinites; CAIs; CB_a; CB_b

* Corresponding author. Laboratoire d'Étude de la Matière Extraterrestre (LEME), Muséum National d'Histoire Naturelle, CP52, 57 rue Cuvier, 75005 Paris, France. Tel.: +33 1 40 79 35 21; fax: +33 1 40 79 57 72.
E-mail address: gounelle@mnhn.fr (M. Gounelle).

0012-821X/$ - see front matter © 2007 Elsevier B.V. All rights reserved.
doi:10.1016/j.epsl.2007.02.007

1. Introduction

Hammadah al Hamra 237 (hereafter HH237), Queen Alexandra Range 94627 paired with Queen Alexandra Range 94411 (hereafter QUE94411) and Mac Alpine Hills 02675 define the CB_b subgroup of the CB chondrite group [2]. CB_b chondrites are enriched in ^{15}N relative to most other chondrite groups ($\delta^{15}N \sim 200‰$), and they exhibit the largest bulk enrichments (depletions) in refractory (volatile) elements relative to CI of all chondrite groups [2]. CB_bs are made mainly of mm-sized metal grains (~70%) and chondrules as well as fragments thereof (~30%). A large fraction of the metal grains are zoned in Ni, Co and PGEs relative to Fe [3–5]. Chondrules are magnesium-rich and have almost exclusively cryptocrystalline and skeletal olivine textures [6]. Minor components are Calcium-, Aluminium-rich Inclusions (CAIs, <1%) [7] and extremely rare heavily hydrated clasts of CI-like composition [8]. In the absence of fine-grained matrix stricto sensu, these components are held together by thin films of impact melts [9].

The large abundance of metal grains, their nearly solar Co/Ni ratio, the reduced silicate mineralogy, and the oxygen isotopic composition of CB_b chondrites are similar to that of Bencubbin, Weatherford and Gujba (CB_a chondrites) [2]. Compared to CB_b chondrites, CB_a chondrites are characterized by the extreme rarity of CAIs [6], larger enrichments in ^{15}N, smaller Ni content of metal, the absence of zoned metal as well as larger chondrule sizes [2]. CB_b chondrites also bear similarities to the metal-rich CH chondrites which contain zoned metal grains [10]. The discovery of the Isheyevo meteorite that contains both CH-like and CB_b-like lithologies further strengthens the link between CH and CB_b chondrites [11]. All these meteorites (CB_as, CB_bs, CHs) form, together with the CR chondrites, the CR clan [12]. The properties of CB_b chondrites, such as the high abundance of metal (~70%), the presence of zoned

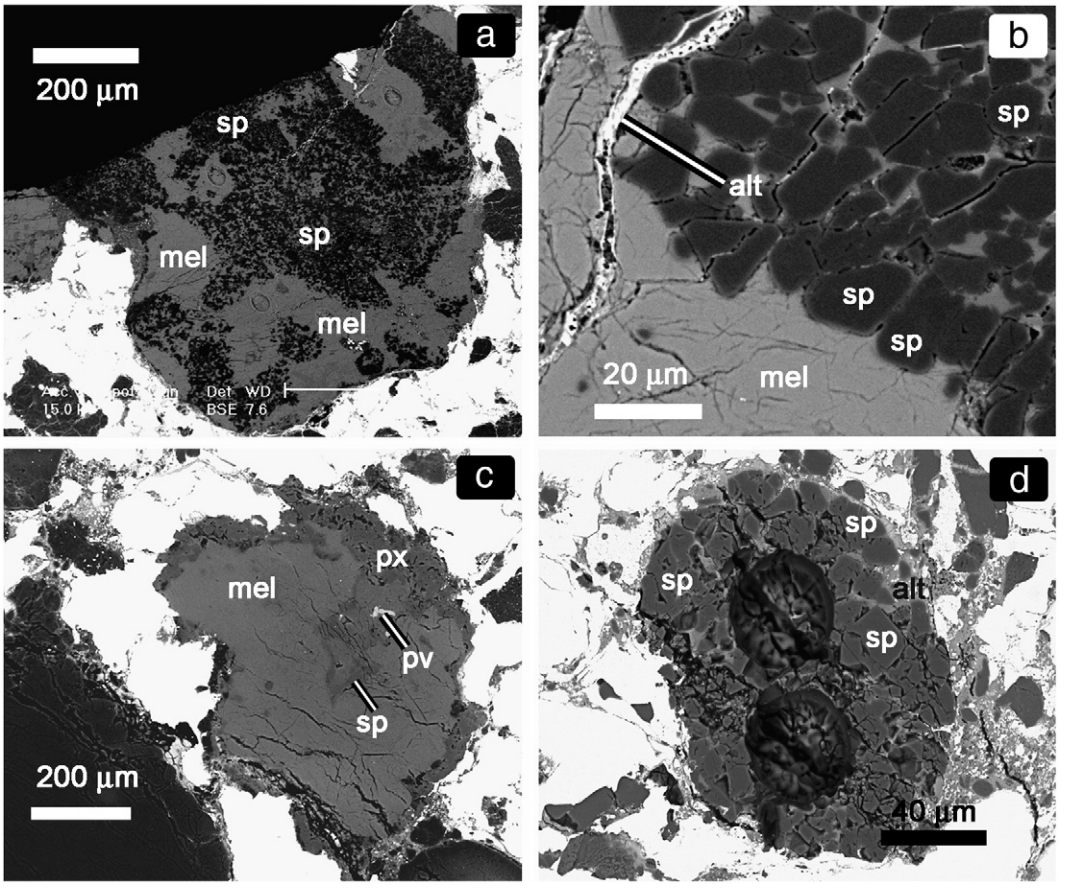

Fig. 1. Backscattered images of CAIs from HH237 and QUE94411. (a) HH237-CAI0 is made of melilite (mel) and spinel (sp) with rare fassaite and extremely rare anorthite. (b) Close-up of HH237-CAI0 showing the relationship between spinel (sp) and melilite (mel). A terrestrial alteration (alt) vein crosscuts the object. (c) QUE94411-CAI1 is made of melilite (mel), Ca-rich pyroxene (px), spinel (sp) and perovskite (pv). (d) QUE94411-CAI2 is made of iron-rich spinel (sp) and a Ca-, Na-rich alteration silicate (alt).

metal, their extreme enrichment (depletion) in refractory (moderately volatile) elements, the absence of fine-grained matrix, and their ^{15}N enrichment distinguish CB_b chondrites from other chondrite groups [13].

The origin of CB_b meteorites is strongly disputed. Rubin et al. [14] suggested that they might result from the impact between two asteroids. Alternatively, Krot and collaborators suggested that CB_b chondrites are extremely primitive, the components of which formed by condensation of a totally vaporized, dusty, region of the solar nebula [15–17]. Because complete vaporization would have required extremely energetic events, Krot et al. [17] proposed that CB_b chondrites formed early in the history of the solar system, when high accretion rates were prevailing in the solar disk. Support for the primitive nature of CB_b chondrites was provided by Weisberg et al. [2] and Campbell et al. [3,4] who pointed out that the chemical composition of CB_b zoned metal grains matches the calculated condensation evolution path in a "canonical" solar nebula.

Recently, the origin of CB_b meteorites has been thrown into upheaval. Using state-of-the art isotopic techniques, Krot and collaborators measured a Pb–Pb age of 4562.8±0.9 Ma for CB_b chondrules, placing their last Pb closure event ~5 Myr after CV3 CAIs [1]. Assuming that accretion disks around young stellar objects fade away on 1–3 Myr timescales, they suggested that CB_b chondrules and metal grains formed in a protoplanetary impact [1], in line with the previous suggestion of Rubin et al. [14]. Implications of this finding are numerous.

First, if CB_b chondrules formed in a protoplanetary impact vapour cloud, they would be the first chondrules for which the formation process had been unambiguously identified, thus providing a benchmark for understanding other chondrule formation mechanisms. Second, if Pb–Pb data record a single event as an impact between two protoplanetary bodies, they can be used to tie relative ages obtained from short-lived radionuclides to an absolute timescale [1].

The aim of the present paper is to report measurements of the magnesium mass-dependent isotopic fractionation of chondrules and CAIs from CB_b chondrites, as well as to provide some constraints on the aluminium-26 content of CAIs at the time of their formation. These data are useful for three reasons. First, they add to the as yet incomplete database on CB_b chondrites for which isotopic measurements are scarce [18–22]. Second, variations in the magnesium isotopic composition record different physical processes such as condensation and evaporation [23], and these new data can potentially constrain the pressure and temperature regime of CB_b chondrule formation (i.e. impact vs. nebular origin). Third, the origins of CAIs in these enigmatic chondrites may be different from that in other chondrite groups, and these differences may be reflected in their Al–Mg isotope systematics as well as their stable magnesium isotopic composition.

2. Samples and experimental methods

We studied two HH237 thick sections (sample BM2000, M9 and sections P12237 and P12241) from the Natural History Museum (NHM, London) and one QUE94411 thick section (QUE94411, 5) allocated to us by the Antarctic Meteorite Working Group (MWG). Scanning electron microscopy was performed

Table 1
Chemical compositions of a diversity of phases in CAIs from HH237 and QUE94411

Meteorite	Object	Na_2O	MgO	Al_2O_3	SiO_2	P_2O_5	SO_2	K_2O	CaO	TiO_2	Cr_2O_3	MnO	FeO	NiO	Total	Mineralogy	# of analyses
HH237	CAI0	bd	27.42	70.87	0.29	bd	bd	bd	0.38	0.53	0.50	bd	0.15	bd	100.14	Spinel	3
HH237	CAI0	bd	0.63	34.68	42.58	bd	bd	bd	19.00	0.05	0.01	bd	1.58	bd	98.52	Anorthite	2
HH237	CAI0	bd	7.44	22.18	35.77	bd	bd	bd	24.45	10.20	0.09	bd	0.49	0.02	100.64	Fassaite	5
HH237	CAI0	bd	3.13	29.14	27.31	bd	bd	bd	40.18	0.07	0.03	bd	0.20	bd	100.05	Melilite	46
QUE94411	CAI1	bd	5.74	23.59	30.68	bd	bd	bd	36.19	1.56	0.02	bd	0.76	bd	98.53	Fassaite	2
QUE94411	CAI1	0.15	13.42	13.37	43.42	bd	bd	bd	23.44	0.37	0.11	0.05	4.04	0.12	98.48	Pyroxene	1
QUE94411	CAI1	0.11	20.12	1.36	50.86	bd	bd	bd	22.03	0.06	0.09	bd	4.28	0.13	99.03	Pyroxene	1
QUE94411	CAI1	0.16	6.86	18.64	32.50	bd	bd	bd	40.02	bd	bd	bd	0.41	0.04	98.62	Melilite	1
QUE94411	CAI1	bd	4.14	27.21	27.65	bd	bd	bd	40.43	0.07	bd	bd	0.52	bd	100.03	Melilite	1
QUE94411	CAI1	0.21	6.48	19.77	31.41	bd	bd	bd	40.72	bd	bd	bd	0.52	bd	99.10	Melilite	1
QUE94411	CAI1	bd	28.51	71.42	0.06	bd	bd	bd	0.04	0.40	0.38	0.06	0.54	bd	101.42	Spinel	1
QUE94411	CAI2	0.25	11.75	19.96	27.68	0.06	0.08	bd	25.16	2.49	0.19	bd	2.21	0.06	89.88	Alteration	1
QUE94411	CAI2	bd	27.73	70.05	0.28	bd	bd	bd	0.14	0.25	0.53	0.03	1.76	0.10	100.86	Spinel	25

bd stands for below detection limit. Data in wt.%.

Table 2
Chemical compostions of a diversity of phases from chondrules of HH237 and QUE94411

Meteorite	Object	Na_2O	MgO	Al_2O_3	SiO_2	P_2O_5	SO_2	K_2O	CaO	TiO_2	Cr_2O_3	MnO	FeO	NiO	Total	Type	Phase	Composition
HH237	R11	bd	53.58	0.14	41.88	0.05	bd	0.03	0.23	bd	bd	bd	4.61	0.03	100.56	SO	Olivine	$Fo_{95.4}$
QUE94411	A1	bd	55.90	0.04	42.38	bd	bd	bd	0.25	bd	bd	bd	1.41	0.04	100.05	SO	Olivine	$Fo_{98.6}$
QUE94411	A1	bd	55.68	0.14	41.85	bd	bd	bd	0.29	bd	bd	bd	1.74	bd	99.76	SO	Olivine	$Fo_{98.3}$
QUE94411	A1	bd	55.86	bd	41.97	bd	bd	bd	0.24	bd	bd	bd	1.53	bd	99.65	SO	Olivine	$Fo_{98.5}$
QUE94411	A1	0.03	55.89	bd	41.95	bd	bd	bd	0.28	bd	bd	bd	1.43	bd	99.61	SO	Olivine	$Fo_{98.6}$
HH237	R1	bd	51.23	0.13	41.05	bd	bd	bd	0.25	bd	bd	bd	6.89	bd	99.60	SO	Olivine	$Fo_{93.0}$
QUE94411	A1	0.19	54.82	0.39	41.95	0.09	bd	bd	0.44	bd	bd	bd	1.47	bd	99.35	SO	Olivine	$Fo_{98.5}$
QUE94411	A1	0.03	55.10	0.18	41.78	0.07	bd	bd	0.35	bd	bd	bd	1.78	bd	99.32	SO	Olivine	$Fo_{98.2}$
HH237	R11	0.06	19.36	17.93	47.04	0.05	0.06	0.03	10.22	bd	bd	bd	5.56	0.44	100.77	SO	Pyroxene	$En_{64.9}Wo_{24.6}$
QUE94411	A10	0.55	30.73	7.30	54.21	0.42	bd	bd	3.28	bd	bd	bd	3.92	0.05	100.50	CC	Pyroxene	$En_{87.1}Wo_{6.7}$
QUE94411	A5	bd	27.75	9.77	52.02	bd	bd	bd	9.10	bd	bd	bd	1.76	bd	100.48	SO	Pyroxene	$En_{78.7}Wo_{18.5}$
HH237	R11	bd	19.87	16.74	45.35	bd	0.04	0.03	9.38	bd	bd	bd	8.56	0.36	100.35	SO	Pyroxene	$En_{63.2}Wo_{21.5}$
QUE94411	A5	bd	36.40	4.55	51.09	bd	0.04	bd	5.02	bd	bd	bd	3.15	0.02	100.33	SO	Pyroxene	$En_{90.0}Wo_{6.5}$
QUE94411	A5	0.04	32.03	4.84	55.42	bd	0.03	bd	5.20	bd	bd	bd	2.42	bd	100.01	SO	Pyroxene	$En_{86.3}Wo_{10.1}$
QUE94411	A5	0.04	26.94	10.26	50.70	bd	0.04	bd	9.89	bd	bd	bd	2.05	bd	99.94	SO	Pyroxene	$En_{76.5}Wo_{20.2}$
HH237	R11	bd	25.65	10.74	49.79	bd	0.05	bd	10.01	0.03	bd	bd	3.09	0.06	99.42	SO	Pyroxene	$En_{74.2}Wo_{20.8}$
QUE94411	A10	0.34	33.91	3.65	55.38	0.06	bd	0.05	2.97	bd	bd	bd	2.67	bd	99.04	CC	Pyroxene	$En_{90.3}Wo_{5.7}$
QUE94411	CH11	bd	44.11	bd	56.41	0.06	bd	bd	0.03	bd	bd	bd	0.98	bd	101.65	CC	Mixture	
QUE94411	CH9	0.04	43.66	0.47	55.91	bd	0.03	bd	0.32	bd	bd	bd	1.03	0.05	101.50	CC	Mixture	
QUE94411	CH7	0.08	41.39	2.88	53.53	0.06	0.05	bd	1.51	bd	bd	bd	0.96	0.04	100.55	CC	Mixture	
QUE94411	A10	0.13	36.96	2.87	54.49	0.08	bd	bd	2.19	bd	bd	bd	2.79	bd	99.55	CC	Mixture	
QUE94411	A7	0.04	36.13	2.94	52.24	0.04	0.05	bd	6.71	bd	bd	bd	0.94	bd	99.11	CC	Mixture	
QUE94411	CH9	0.21	41.30	1.39	52.37	0.14	0.13	bd	0.50	bd	bd	bd	1.82	0.09	97.96	CC	Mixture	
QUE94411	A10	0.09	34.90	2.77	50.17	0.18	0.03	bd	2.08	bd	bd	bd	6.23	0.19	96.65	CC	Mixture	
HH237	R1	0.12	4.98	21.59	54.98	0.05	0.06	bd	16.01	0.03	bd	bd	1.05	bd	98.89	SO	Mesostasis	
HH237	R1	bd	38.68	5.85	45.37	0.03	bd	bd	4.61	bd	bd	bd	4.12	bd	98.72	SO	Mesostasis	
QUE94411	A1	0.07	4.99	21.93	50.29	0.03	0.05	bd	18.02	0.06	bd	bd	0.39	bd	95.83	SO	Mesostasis	
QUE94411	A1	0.10	4.05	20.07	46.24	bd	0.03	bd	16.00	0.04	bd	bd	0.57	bd	87.14	SO	Mesostasis	

bd stands for below the detection limit. Data in wt.%.

at London, Orsay and Paris. Mineral compositions were obtained at the Service Commun de Microscopie (CAMPARIS — Université Paris 6) with a CAMECA SX100 Electron Microprobe (EMP) operated at a 15 keV acceleration voltage and a 10 nA current. Detection limit of all oxides is ~0.02 wt.%.

Magnesium isotopic analyses were carried out in three different sessions (March, October and November 2005) at UCLA, using 193 nm laser ablation combined with multiple-collector inductively coupled plasma-source mass spectrometry (MC-ICPMS, ThermoFinnigan Neptune) following the sample-standard bracketing method [24,25]. Laser spot size was between 55 and 100 μm and laser pulse repetition rates varied between 1 and 2 Hz, depending on the magnesium content of the considered phase. Laser fluences varied between 20 and 25 J/cm^2. Ablation was carried out in pure He gas with a flow rate of ~0.5 l/min. Ablation products were delivered to the source of the MC-ICPMS instrument following mixing with Ar gas (~0.5 l/min). The magnesium isotopic composition is reported relative to the DSM3 standard [26] using the δ^iMg′ notation with $\delta^i Mg' = 1000 \times \ln((^iMg/^{24}Mg)_{sample}/(^iMg/^{24}Mg)_{DSM3})$, i representing the masses 25 and 26. The linear (i.e., logarithmic) form of the delta values facilitates accurate calculation of excess magnesium-26 [23]. Differences with the more commonly used δ^{25}Mg and δ^{26}Mg is however extremely small (~0.05‰ for δ^{25}Mg=10‰ [27]). When we compare literature data to our own data, we use both δ^{25}Mg′ and δ^{25}Mg. On the DSM3 scale, chondrites have $\delta^{25}Mg' \sim \delta^{26}Mg' \sim 0$. Magnesium-26 excesses due to the decay of ^{26}Al, hereafter δ^{26}Mg*, are calculated as $\delta^{26}Mg^* = \delta^{26}Mg' - \delta^{25}Mg'/\beta$ where β=0.521. The use of β=0. 521 for the mass-dependent fractionation law, implying an equilibrium processes, instead of β=0. 511, a likely minimum for a purely kinetic processes affecting Mg, or β=0.516 (the often-cited value for Rayleigh fractionation), does not change the value of δ^{26}Mg* in this study because δ^{25}Mg′ and δ^{26}Mg′ are sufficiently close to zero as to render the influence of the exact value for β negligible [27]. External reproducibility is estimated to be ~±0.25‰/amu (2σ) from repeated analyses of mineral standards [24,25]. Errors on δ^{26}Mg* for CAIs are between 0.1 and 0.2‰.

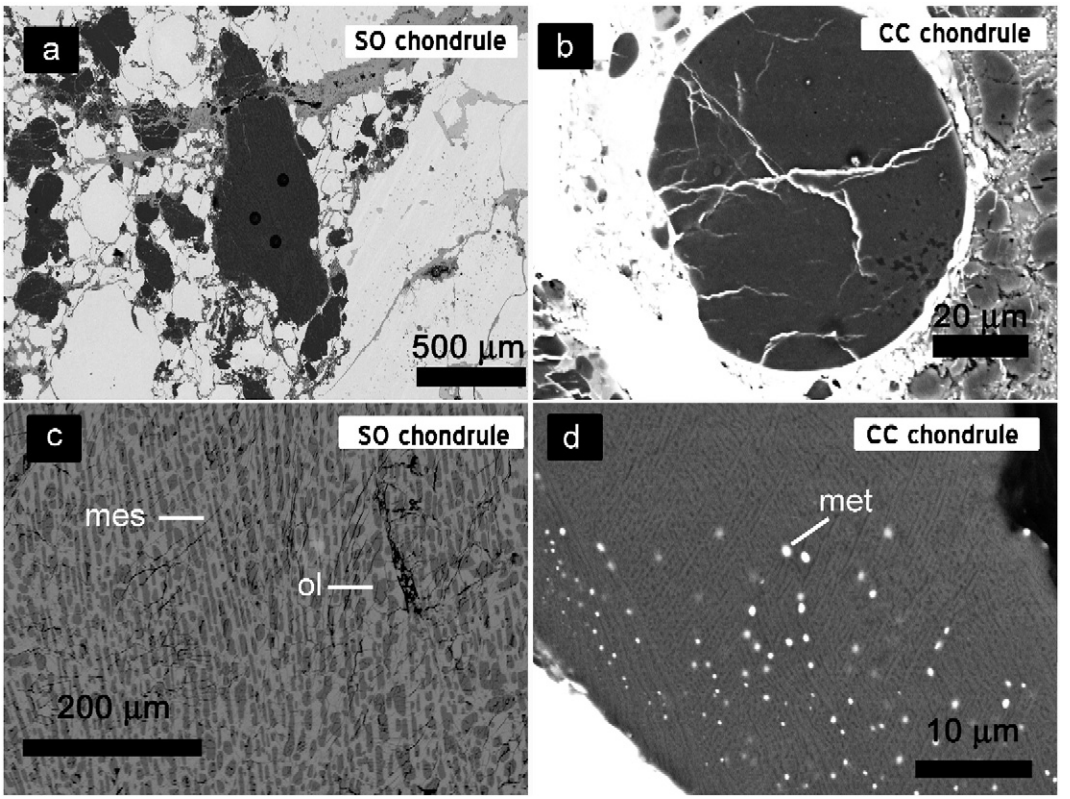

Fig. 2. Backscattered images of chondrules from HH237 and QUE94411 (a) Typical SO chondrule from HH237-J. (b) Typical CC chondrule from HH237-R. (c) Close-up of the SO texture. Olivine (ol) is enclosed in a glassy mesostasis (mes). (d) Close-up of the CC texture. Radiating unidentified minerals and nickel-free iron metal (met) are set up in a silica-rich matrix.

3. Results

3.1. Mineralogy

HH237-CAI0 is a compact object made of melilite and spinel with rare fassaite and extremely rare anorthite (Fig. 1a,b and Table 1). It has some cracks and unidentified alteration products, possibly formed during terrestrial residence. Akermanite (Ak) content in melilite varies from 0.2 to 37.4 mol.% (Ak=23.0 mol.%, average of 46 analyses, where Ak is calculated as the average of $(1-Al/2)*100$ and $(Si-1)*100$ with Al and Si being the number of aluminium and silicon atoms relative to 7 oxygen atoms). Spinel has significant CaO (up to 0.48 wt.%), TiO_2 (up to 0.57 wt.%), Cr_2O_3 (0.50 wt.%) and low FeO (0.17 wt.%). Fassaite has TiO_2 contents ranging from 7.5 to 12.5 wt.% (total Ti as TiO_2). Because of the spinel small size, some of the minor elements such as Ca could be a contamination from the surrounding melilite.

QUE9441-CAI1 is a compact object made of melilite, diopside with varying amount of Al_2O_3 and TiO_2, minor spinel and rare perovskite (Fig. 1c, Table 1). The akermanite content of melilite varies from 19.2 to 61.4 mol.%, although no clear zoning has been observed. TiO_2 content of fassaite is 9.8 wt.% (average of two analyses). Spinel is low in FeO (0.54 wt.%).

QUE94411-CAI2 is a relatively fine-grained inclusion made of euhedral spinel and alteration phases (Fig. 1d, Table 1). The iron content of spinel is high (FeO up to 3.4 wt.%, average 1.8 wt.%). The alteration phase is an iron magnesium silicate enriched in Ca and Na. It probably results from the alteration of the mesostasis.

Though there is no definitive evidence, we contend that the CB_b CAIs we studied are of igneous origin. CAIs in our study are similar to those described by Krot et al. [7] who report pyroxene±spinel±melilite objects as the most common CAIs occurring in CB_b chondrites. The compact texture and the euhedral spinel shape of

Table 3
Magnesium isotopic compositions of CAIs and chondrules from HH237 and QUE9441

Meteorite	Object	Analysis	$\delta^{25}Mg'$	σ_m	$\delta^{26}Mg'$	σ_m	$^{27}Al/^{24}Mg$	σ_m	$\delta^{26}Mg^*$	σ_m	Mineralogy [a]
HH237	CAI0	O3	1.31	0.04	2.23	0.06	4.10	0.12	−0.32	0.08	Melilite
HH237	CAI0	O4	0.32	0.11	0.42	0.19	6.41	0.21	−0.20	0.25	Melilite
HH237	CAI0	O5	0.41	0.10	0.86	0.09	7.16	0.13	0.07	0.21	Melilite
HH237	CAI0	O6	0.69	0.07	1.44	0.06	2.47	0.01	0.10	0.09	Spinel
HH237	CAI0	O7	0.70	0.05	1.38	0.05	4.54	0.04	0.03	0.11	Melilite
HH237	CAI0	O8	0.78	0.09	1.10	0.11	2.17	0.02	−0.42	0.12	Spinel
HH237	CAI0	O9	0.54	0.07	1.15	0.15	5.11	0.19	0.10	0.16	Melilite
HH237	CAI0	O12	−0.03	0.07	−0.09	0.09	0.99	0.07	−0.03	0.11	Melilite near edge
QUE94411	CAI1	N3	0.84	0.06	1.83	0.10	2.04	0.03	0.19	0.11	Melilite
QUE94411	CAI1	N6	0.79	0.05	1.80	0.14	2.66	0.04	0.26	0.17	Melilite
QUE94411	CAI2	N2	0.02	0.07	0.01	0.08	1.94	0.01	−0.03	0.10	Spinel
QUE94411	CAI2	N8	0.09	0.13	0.00	0.15	1.98	0.01	−0.17	0.16	Spinel
HH237	R1	O1	0.15	0.07	−0.05	0.11	0.24	0.01	−0.34	0.12	SO
HH237	R1	O10	0.33	0.07	0.47	0.06	0.28	0.01	−0.16	0.14	SO
HH237	R11	O11	0.15	0.07	0.13	0.06	0.24	0.00	−0.16	0.08	SO
HH237	J2	M2	0.06	0.08	0.10	0.05	0.07	0.00	−0.02	0.12	SO
HH237	J3	M3	0.62	0.11	1.18	0.07	0.28	0.00	−0.03	0.16	SO
HH237	J3	M4	0.45	0.11	0.81	0.11	0.25	0.02	−0.06	0.12	SO
HH237	J5	M5	0.95	0.18	1.64	0.13	0.35	0.01	−0.21	0.24	SO
HH237	J5	M6	0.62	0.09	1.07	0.09	0.49	0.01	−0.14	0.14	SO
HH237	J5	M7	0.63	0.22	1.01	0.12	0.41	0.02	−0.22	0.30	SO
HH237	J9	M9	0.28	0.19	0.48	0.11	0.18	0.00	−0.07	0.27	CC
HH237	J10	M10	0.26	0.20	0.18	0.10	0.12	0.00	−0.32	0.28	CC
QUE94411	A1	N1	0.37	0.07	0.47	0.07	0.34	0.01	−0.25	0.13	SO
QUE94411	A4	N4	0.02	0.09	0.07	0.12	0.00	0.00	0.03	0.21	SO
QUE94411	A5	N5	0.60	0.08	1.00	0.10	0.20	0.00	−0.16	0.11	SO
QUE94411	A7	N7	−0.07	0.08	−0.55	0.12	0.07	0.00	−0.41	0.12	CC
QUE94411	A9	N9	−0.35	0.09	−0.94	0.21	0.01	0.00	−0.26	0.09	CC
QUE94411	A12	N12	−0.49	0.07	−1.21	0.07	0.01	0.00	−0.26	0.16	CC
QUE94411	A10	N10	−0.15	0.07	−0.45	0.14	0.09	0.00	−0.15	0.12	CC
QUE94411	A11	N11	−0.80	0.07	−1.50	0.12	0.00	0.00	0.06	0.11	CC

The delta values and their associated errors are expressed in ‰.

[a] For CAIs, we indicate the main mineral ablated. For chondrules, we indicate the type (SO or CC). In the case of chondrules, individual phases are always too small to be analyzed as such.

HH237-CAI0 suggest it crystallized from a melt (Fig. 1b). The texture of QUE94411-CAI2 is similar to that of a chondrule with euhedral spinels enclosed in a (now altered) mesostasis, indicative of an igneous nature. The compact texture of QUE94411-CAI1 is somehow insufficient to demonstrate it has an igneous origin. Based on crystallization experiments [28], it was however demonstrated that the bulk chemistry as well as the petrography of pyroxene±spinel± melilite CB_b CAIs is compatible with crystallisation from a melt [7]. We will therefore consider that the CB_b CAIs studied here are of igneous origin, as originally suggested by Krot et al. [7].

Analyzed chondrules are similar to the typical skeletal olivine (SO) and cryptocrystalline (CC) chondrules previously described in CB_b chondrites [6]. SO chondrules consist of olivine grains with variable compositions set up in a glassy mesostasis (Table 2, Fig. 2). Cryptocrystalline chondrules are very fine-grained that make them difficult to analyze with present analytical techniques. They are silica-rich and occasionally contain nickel-free iron metal beads (Table 2, Fig. 2).

3.2. Mg isotopic composition

In HH237-CAI0, $\delta^{25}Mg'$ varies from -0.03 ± 0.07‰ (1σ) to 1.31 ± 0.04‰ (1σ) and $\delta^{26}Mg'$ varies from -0.09 ± 0.09‰ (1σ) to 2.23 ± 0.06‰ (1σ) (Table 3 and Fig. 3). All data fall on the terrestrial fractionation line. No significant excess of ^{26}Mg was found, indicating that ^{26}Al was not extant when the Mg–Al system closed in

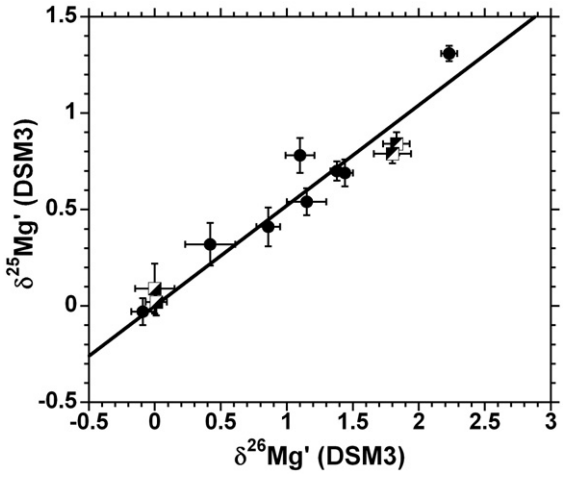

Fig. 3. Mg isotopic composition of CAIs. Filled circles are HH237-CAI0. Squares (black triangle upward) are QUE9411-CAI1. Squares (black triangle downward) are QUE94411-CAI2. Black line is the terrestrial fractionation line (TFL).

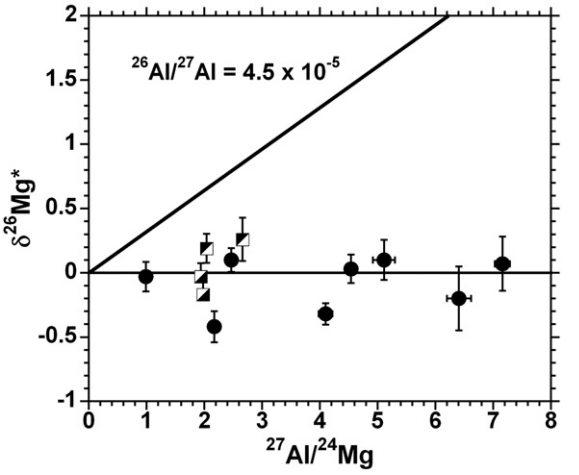

Fig. 4. Al–Mg isochron diagram for CAIs. Filled circles are HH237-CAI0. Squares (black triangle upward) are QUE9411-CAI1. Squares (black triangle downward) are QUE94411-CAI2. The $^{26}Al/^{27}Al = 4.5\times10^{-5}$ line is shown for reference.

HH237-CAI0. The data are sufficient to place an upper limit on the initial $^{26}Al/^{27}Al$ ratio for this object of 8.0×10^{-6}. No mineralogical control was observed on the mass dependent isotopic fractionation in the CAI.

Because CAIs from QUE94411 are small, only two data points were acquired for each inclusion (Fig. 3). The $\delta^{25}Mg'$ and $\delta^{26}Mg'$ average values from QUE94411-CAI1 are 0.82 ± 0.08‰ and 1.81 ± 0.18‰ (1σ) respectively. The average $\delta^{25}Mg'$ and $\delta^{26}Mg'$ from QUE94411-CAI2 are 0.05 ± 0.15‰ and 0.00 ± 0.17‰ (1σ) respectively. All data fall on the terrestrial fractionation line within uncertainties. No detectable excess of ^{26}Mg was found in either inclusion, indicating that the concentration of ^{26}Al was negligible when QUE94411 CAIs crystallized. The spread in $^{27}Al/^{24}Mg$ (from 1.94 to 2.66) is too small to calculate a rigorous upper limit for the $^{26}Al/^{27}Al$ ratio for these objects based on the slope in the Al–Mg evolution diagram.

Regression of all three CB_b CAIs together (i.e. putting the HH237 CAI together with the two CAIs of QUE 94411), results in an upper limit for the initial $^{26}Al/^{27}Al$ ratio for these objects of 4.6×10^{-6} (Fig. 4).

Chondrules from HH237 have $\delta^{25}Mg'$ and $\delta^{26}Mg'$ varying from 0.06 ± 0.08 to 0.95 ± 0.18‰ (1σ), and from -0.05 ± 0.11 to 1.64 ± 0.13‰ (1σ) respectively. Chondrules from QUE94411 have $\delta^{25}Mg'$ and $\delta^{26}Mg'$ varying from -0.80 ± 0.07 to 0.60 ± 0.08‰ (1σ), and from -1.50 ± 0.12 to 1.0 ± 0.10‰ (1σ) respectively. All data fall on the terrestrial fractionation line within uncertainties (Fig. 5). There is no intrachondrule variation at the 2σ level (Table 3). Note that, given the analytical

precision of the laser ablation method and the low $^{27}Al/^{24}Mg$ ratio of chondrules (<0.5), even a canonical or supracanonical $^{26}Al/^{27}Al$ would be undetectable. The reported data therefore do not constrain the initial $^{26}Al/^{27}Al$ ratio of the chondrules.

4. Discussion

4.1. Chondrules

4.1.1. Mixing, evaporation and condensation

Fig. 6 shows the relationship between the $\delta^{25}Mg'$ and the $^{24}Mg/^{27}Al$ ratios of chondrules. The observed rough negative correlation can result from evaporation (concomitant enrichment of the Al/Mg ratio and the $\delta^{25}Mg'$ due to the more refractory nature of aluminium compared to magnesium), or by mixing between a magnesium unfractionated, aluminium-poor end member (matrix) and a fractionated, aluminium-rich end member such as a CAI. CB_b chondrules roughly fall on a curve proposed by Galy et al. [29] defined by Allende chondrules and the Allende CAI AG178 (Fig. 6). Note that Allende chondrules recently measured by Bizzarro et al. [30] also fall on the Galy et al. curve (Fig. 6). If the curve is due to mixing, it means that CV3 and CB_b chondrules result from the mixing of two identical end-members, one of which was similar to Allende CAI AG178. In so far as the Mg/Al of AG178 is not representative of all CAIs, the mixing scenario seems unlikely. An alternative is that the curve is the result of evaporation under conditions that prevent substantial Mg isotope fractionation.

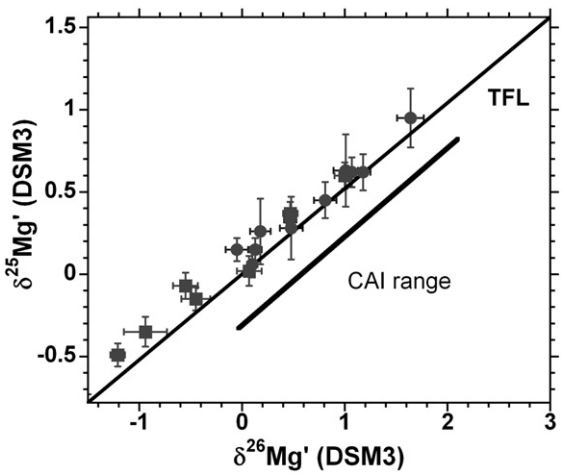

Fig. 5. Mg isotopic composition of chondrules. Full grey squares are QUE94411 chondrules. Filled grey circles are HH237 chondrules.

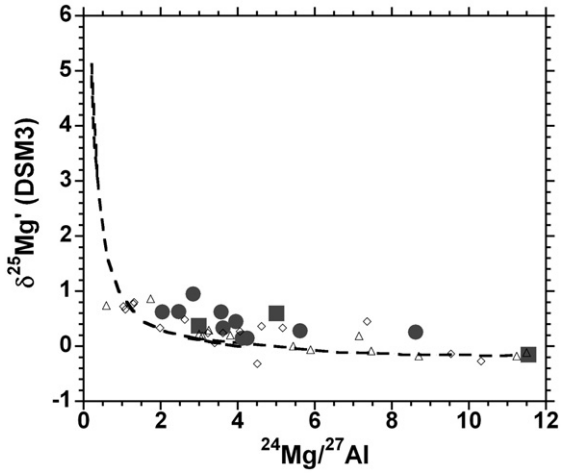

Fig. 6. $\delta^{25}Mg'$(DSM3) vs. $^{24}Mg/^{27}Al$ for chondrules. Full grey squares are QUE94411 chondrules. Filled grey circles are HH237 chondrules. Some QUE9441 chondrules were omitted for the sake of clarity (containing virtually no aluminium, they plot on the far right). Open diamonds are Allende (CV3) chondrules from Bizzaro et al. (2002) [30]. Open triangles are Allende (CV3) chondrules from Galy et al. (2000) [29]. The dashed thick line is the Allende (CV3) mixing line between the CAI AG178 and matrix [29].

4.1.2. The low mass-dependent fractionation of chondrules

CB_b chondrules exhibit a similar mass fractionation range as Allende chondrules, i.e. they have $\delta^{25}Mg'$ varying from −0.80 to 0.90‰ (this work) while Allende chondrules have $\delta^{25}Mg'$ varying from −0.32 to 0.86‰ [29,30]. The similarity in the Mg isotopic composition of QUE94411 and HH237 (CB_bs) and Allende (CV3) chondrules is striking in view of their numerous differences in term of mineralogy and chemistry [1,17]. Lunar spherules, although different in mineralogy, bear some textural similarities with chondrules [31], and also show little evidence for magnesium mass dependent fractionation [32]. It seems, therefore, a general observation that round, once-molten, silicate spheres evaporated (as suggested by variable Mg/Al) in physical conditions such that magnesium isotopic fractionation was suppressed. Two possibilities have been envisioned for suppressing magnesium isotopic fractionation during evaporation: evaporation at high magnesium partial pressure or at high total gas pressure [23]. The first possibility can result if chondrules formed in close proximity to each other [23,33], and the second results if the evaporating gas remains closely bound to its parent chondrule by virtue of slow diffusion through a high background number density of H_2 [34]. Although the rough negative correlation between $\delta^{25}Mg'$ and the $^{24}Mg/^{27}Al$ ratio (Fig. 6) might shed light on the

chondrule-forming mechanisms, it is difficult to distinguish between these two possibilities at present. Because radically different types of chondrules as well as lunar impact spherules show similar limited mass dependent magnesium isotope fractionation, these data offer little constraint on the origin of CB_b chondrules.

4.2. CAIs

4.2.1. The low mass-dependent fractionation of CAIs

CAIs in CB_b chondrites exhibit limited mass-dependent fractionation, with two of the three CAIs analyzed having slightly higher $^{25}Mg/^{24}Mg$ ratios than chondrites (DSM3). The average $\delta^{25}Mg'$ of all CAIs data points is 0.54‰. This enrichment in the ^{25}Mg isotope is modest in comparison to igneous CAIs overall [35].

Although recent high precision work has considerably improved our knowledge of CAIs magnesium isotopic composition, it is not yet clear what the magnesium isotopic composition of igneous CAIs in CV3 chondrites is as a group. While the UCLA laboratory [24,25] consistently reports high $\delta^{25}Mg'$ values for igneous CAIs (few to 8‰), the Copenhagen laboratory reports a wide range of isotopic compositions for igneous CAIs (we retained as igneous CAIs the ones labelled type B by [30]). Out of 11 igneous CAIs analyzed by [30,36], 5 are high in $^{25}Mg/^{24}Mg$ ($\delta^{25}Mg > 2$‰ on the DSM3 scale), 6 have little mass-dependent fractionation ($\delta^{25}Mg$ between −1 and +1‰) and 1 is low in $^{25}Mg/^{24}Mg$ ($\delta^{25}Mg = -1.94$‰). Data from the Chicago group [37] are consistent with those of UCLA; eleven igneous CAIs (type B or compact type A, considering E13 as a type A CAI [38]) out of the twelve measured by Simon et al. [37] have high $\delta^{25}Mg$ relative to the DSM3 standard ($\delta^{25}Mg > 1.25$‰). Only E62 is low in $^{25}Mg/^{24}Mg$ ($\delta^{25}Mg = -1.25$‰).

The difference between the Copenhagen data set and the Chicago and Los Angeles data sets can be further appreciated when looking at Fig. 7. The differences could be due either to a lack of statistically significant sampling, discrepancies in CAI categorization, admixture of light matrix material into CAIs while microdrilling polished slabs or a combination of all three possibilities. We observe that among the igneous CAIs measured in Copenhagen and having a low $^{25}Mg/^{24}Mg$ ratio, all but one have low $^{27}Al/^{24}Mg$ ratios compared to typical Allende igneous CAIs. The $^{27}Al/^{24}Mg$ of CV3 CAIs measured by the Copenhagen group [30,36] varies from 0.09 to 3.4 (average 1.7) using MC-ICPMS (with 2% relative precision) while values for CV3 CAIs reported by Simon et al. [37] and measured by INAA have $^{27}Al/^{24}Mg$ ratios of 1.6 to 5.3 (average 2.4) [38]. Based on these observations, we will conclude that igneous CV3 CAIs generally have high $\delta^{25}Mg'$ ($\delta^{25}Mg' > 1.25$‰) relative to chondrite (DSM3).

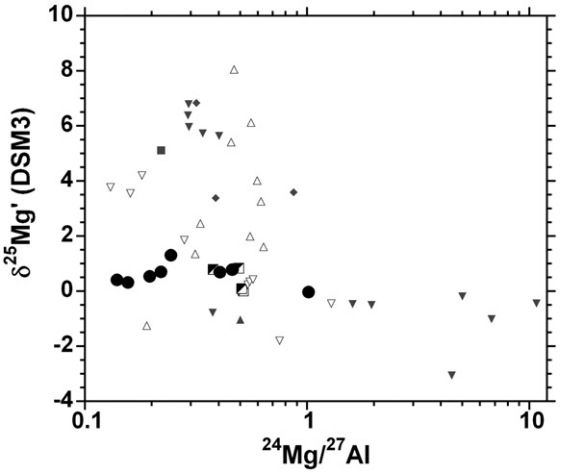

Fig. 7. $\delta^{25}Mg'$(DSM3) vs. $^{24}Mg/^{27}Al$ for CAIs. Filled circles are HH237-CAI0. Squares (black triangle upward) are QUE9411-CAI1. Squares (black triangle downward) are QUE94411-CAI2. Upper triangle, square, lower triangle and diamond are CV3 CAIs data from the Chicago group [37, 38], Galy et al. [29], the Copenhagen group [30, 36] and the UCLA group [25] respectively. Filled symbols are igneous CAIs. Open symbols are non-igneous CAIs.

Given that typical igneous CAIs in CV3 meteorites have high $\delta^{25}Mg'$, the low $\delta^{25}Mg'$ of igneous CAIs in CB_b chondrites ($\delta^{25}Mg' < 1.3$‰) stands out as an important feature. These observations suggest that CB_b CAIs formed in a physical environment unlike that of igneous CV3 CAIs. The nearly chondritic $^{25}Mg/^{24}Mg$ of CB_b CAIs suggests further that these objects may have formed in a region of higher total gas pressure or higher magnesium partial pressure that prevented free evaporation of Mg while the CAIs were in the molten state.

4.2.2. The non-detection of ^{26}Al in CB_b CAIs

CAIs in CB_b chondrites did not contain appreciable ^{26}Al when the Al–Mg system closed ($^{26}Al/^{27}Al < 4.6 \times 10^{-6}$). The question is whether CB_b CAIs contained ^{26}Al when they first formed, or whether the absence of ^{26}Al is due to secondary event(s) provoking the redistribution of the Mg isotopes and erasing a putative record of aluminium-26 decay. Our Mg isotope data suggest that the CB_b CAIs did not contain ^{26}Al when they first formed and that the lack of $^{26}Mg^*$ is not the result of diffusive reequilibration in CB_b CAIs. The intercept $\delta^{26}Mg^*_0$ of the Al–Mg evolution line (see Fig. 4) is zero within error (-0.12 ± 0.10‰, 2σ) for HH237-CAI0, suggesting it first formed without much ^{26}Al.

For example, if HH237-CAI0 had formed with an initial $^{26}Al/^{27}Al$ of 4.5×10^{-5}, and magnesium isotopic redistribution occurred in a closed system (i.e. within the CAI itself, e.g. [25,39]), $\delta^{26}Mg^*_0$ should be equal to $10^3\times(^{26}Al/^{27}Al)_0/0.13982\times(^{27}Al/^{24}Mg)_{bulk}$. This CAI is made essentially of spinel ($^{27}Al/^{24}Mg=2.53$) and melilite with $^{27}Al/^{24}Mg$ larger than 4.7, meaning that its $(^{27}Al/^{24}Mg)_{bulk}$ is certainly greater than 2. HH 237 CAI0 should have, therefore, a minimum $\delta^{26}Mg^*_0$ of 0.644‰, which is clearly not the case. On this basis it seems this CB_b CAI did not contain ^{26}Al when it first formed and one can infer from this that the lack of $^{26}Mg^*$ is not the result of diffusive reequilibration in CB_b CAIs in general. This conclusion is supported by petrographic observations that show little alteration of CB_b CAIs (see also [7]), while CV3 CAIs for which the Al–Mg is so clearly disturbed show clear evidence for secondary heating and sometimes remelting [40].

The absence of ^{26}Al in CB_b CAIs is reminiscent of the situation observed in the closely related CH chondrite group [41]. In the Acfer 182 CH chondrite, 17 CAIs out of 18 are devoid of ^{26}Al. There are three possible interpretations for the genuine absence of ^{26}Al in CAIs; (1) CAIs with no ^{26}Al could have formed extremely early, before ^{26}Al injection by a star such as a supernova [42]; (2) CAIs with no ^{26}Al could have formed late, i.e. 2.7 Myr (for $^{26}Al/^{27}Al<4.6\times10^{-6}$) after those CAIs that formed with a supercanonical $^{26}Al/^{27}Al$ ratio of 6×10^{-5}; and (3) CAIs in CB_b chondrites were never exposed to impulsive flares, assuming an irradiation origin for ^{26}Al [43,44]. The first two possibilities rely on the assumption of an homogeneous distribution of ^{26}Al, usually associated with a stellar origin for ^{26}Al [45]. In the third case, different amounts of ^{26}Al in different primitive objects reflect only different levels of irradiation, and have no chronological meaning [46,47].

If CB_b CAIs formed before injection of aluminium-26 by a supernova, they were either free floating in the solar accretion disk for ~5 Myr (the difference between the Pb–Pb ages of CB_b chondrules and CAIs) or were stored in a parent-body for a similar time span. Because the residence time of 100 μm CAIs in the solar accretion disk is $\sim10^6$ yr [48], the former possibility is unlikely. Even if turbulence keeps them free-floating in the solar accretion disk [49], it is difficult to understand why common porphyritic chondrules were not delivered to the impact plume together with CAIs, since these are much more common chondritic components than CAIs [50]. In addition, the observation that each chondrite group has its own set of chondrules in term of texture, mineral composition or size argues for the absence of mixing on the scale of the disk on large timescales.

CB_b CAIs thus formed extremely early (before ^{26}Al injection) only if they were stored in a parent-body for at least 4.4 Myr. In the context of a collisional origin for CB_b meteorites, the CB_b CAIs belonged either to the impactee or the impactor and survived the impact, as first suggested by Wasson (personal communication), by analogy to the proposed history of CH chondrites [51]. Krot et al. suggest that CAIs were remelted in close proximity to the CB chondrule-forming region [6], i.e. in the impact plume. This is however incompatible with the oxygen isotopic composition data. The low temperature limit in the chondrule-forming region is estimated to be 1800 K [6]. At that temperature, a 400 μm CAI takes only a few hours to equilibrate its original oxygen isotopic ($\delta^{17}O_{SMOW}\sim\delta^{18}O_{SMOW}\sim-50$‰) composition with the ambient gas ($\delta^{17}O_{SMOW}\sim\delta^{18}O_{SMOW}\sim0$‰) if one assumes a liquid diffusion coefficient of $D\sim1.9\times10^{-8}$ and the relationship $t=L^2/D$. This timescale is probably far shorter than the chondrule formation timescale [6]. It is undoubtedly shorter by one to two orders of magnitude than the zoned metal formation timescale [5]. As CB_b CAIs have an oxygen isotopic composition different from that of CB_b chondrules [7], we conclude therefore that CB_b CAIs were not remelted in the putative impact cloud. Given the estimated minimum temperature of the collision plume (>1800 K), our conclusion casts some doubt on the existence of such a cloud.

We showed above that it is unlikely CB_b CAIs formed early in the history of the solar accretion disk. We therefore favour possibilities (2) and (3) for the formation of CB_b CAIs. In case (2) which assumes a straightforward chronological meaning for aluminium-26, CAIs formed late. In case (3), the absence of aluminium-26 indicates a lack of exposure to impulsive flares which generates aluminium-26 through ^3He and proton irradiation [43]. In the chronological model developed by [46], compatible with an irradiation origin of aluminium-26, CB_b CAIs are expected to form at the same time as CB_b chondrules, i.e. some Myr after CV3 CAIs. If CAIs formed late, assuming that CAIs are formed in a disk [52], it means that a solar accretion disk still existed when they formed. If a solar accretion disk was able to generate CAIs, it might also have generated chondrules.

4.3. Chondrule formation and accretion disk timescales

The main argument for a giant impact origin for CB_b chondrules is their young age [1], as well as their single stage formation [6]. The suggestion is that CB_b chondrules formed 5 Myr after the CV3 CAIs, and that this long timescale is incompatible with an accretion disk origin as infrared excesses in the spatial energy

distributions of young solar-mass stars disappear over a timescale of 1–3 Myr.

Two aspects of the argument for a giant impact origin for CB_b chondrules are disputable. First, the measured Pb–Pb age of CB_b chondrules is 4562.8±0.9 Ma [1] while CV3 CAIs best age is 4567.2±0.6 Ma [53]. We note that the chondrule age is a weighted average of different ages, and that its precision may therefore be overestimated. Nonetheless, even at face value, these data mean that the difference between CB_b chondrules and the oldest CV3 CAI is 4.4±1.5 Ma. This is less than the 5 Myr quoted in Krot et al. [1]. Indeed, error bars also allow the time difference to be as little as 2.9 Myr. A common view, based on the assumption that ^{26}Al was homogeneously distributed in the solar accretion disk and can be used as a fine-scale chronometer [54], is that most chondrules from a diversity of carbonaceous and ordinary chondrites groups formed later than a few Myr after CV3 CAIs (see e.g. Fig. 3c of [55]). This late formation of carbonaceous and ordinary chondrites chondrules never before raised the question of the longevity of the solar circumstellar disk. If the minimum age separation of 3 Myr is too long for CB_b chondrules to have formed in the nebula, then one is forced to argue that chondrules from other chondrite groups also did not form in the nebula.

In addition, we point out that some low-mass stars still have a disk after 3 Myr of evolution. Roughly 60% of the stars from the η Chameleontis cluster (~9 Myr old) have an accretion disk [56]. In the three clusters NGC 2264, NGC 2362, and NGC 1960, only half of the disks disappear on a 3 Myr timescale, and the overall disk lifetime is estimated to be ~6 Myr [57], well within the 4.4 Myr interval obtained for the CB_b chondrules and CV3 CAIs. One should keep in mind that the abundance and lifetime of disks are lower limits, since observation capabilities detect only dust of a limited size and temperature [58]. We are not arguing that all solar-mass stars still possess a disk after 4.4 Myr of evolution, only that a significant fraction of them do. It is incorrect to argue that the relatively young age (4.4±1.5 Ma after CV3 CAIs) of CB_b chondrules is a proof of a giant impact origin on the basis that there was no longer an accretion disk.

Because CB_b chondrules are not that old (the lower limit of their age difference with CV3 CAIs is only 2.9 Myr), and because accretion disks can survive a lot longer than 1–3 Myr as argued by Krot et al. [1], there is no strong need for a giant impact origin for CB_b chondrules. Other arguments put forward by [1], i.e. the lack of fine-grained interchondrule matrix had been interpreted previously by the same authors as an indication of the primitiveness of CB_b chondrites [9].

5. Summary and speculations

Our Mg isotope data for CB_b chondrules shows that they are similar to many other once-molten millimeter, silicate-rich spherules in the solar system, having nearly chondritic $^{25}Mg/^{24}Mg$ ratios. These data permit either a nebular or a collisional origin. Although the peculiar chemical, petrographic and mineralogic properties of CB_b chondrules are compatible with a condensation origin, the precise astrophysical setting could be either an impact vapour cloud [1] or the solar accretion disk [17]. We note, however, that the formation of relatively young chondrules in a solar accretion disk is not incompatible with the astronomical observations of young stellar objects, contrary to the claim of [1].

The magnesium isotopic composition of CB_b CAIs is a stronger constraint for the origin of CB_b chondrites. Their lack of magnesium mass dependent isotope fractionation and absence of ^{26}Al during their formation, in addition to their ^{16}O-poor nature (relative to other CAIs), distinguish them from CV3 CAIs. We suggest that CB_b CAIs did not form early in the history of the solar system, and favour instead, on the basis of lack of ^{26}Al, either a late origin, assuming a chronological meaning for aluminium-26, or formation in the absence of impulsive flares in the evolving Sun that may have produced ^{26}Al. In the latter case, we contend for consistency that CB_b CAIs formed contemporaneously with CB_b chondrules. Because, as far as we know, a solar accretion disk is needed to make CAIs, and lacking clear evidence that a collision would produce CAIs, there is no reason to assume that a late date of origin for CB_b CAIs is indicative of a collisional origin for CB_b chondrites. The young age of CB_b CAIs may comprise instead a strong constraint on the longevity of the solar accretion disk. The low magnesium mass dependent fractionation of CB_b CAIs might be indicative of an environment with higher total gas pressures than the environment where CV3 CAIs formed.

We propose, in line with the ideas proposed by [46,47], that the data for both CAIs and chondrules of CB_b chondrites are consistent with their formation in the solar accretion disk, and that they were brought together to form parts of the CB_b parent body possibly by a x-wind mechanism [59]. Based on Pb–Pb ages, CB_b components formed late comparatively to CV3 chondrites. In such a scenario, the differences observed between CB_b chondrites and e.g. CV3 chondrites can be ascribed to physical changes with time of the solar accretion disk. The rarity of CAIs and their lack of aluminium-26 in CAIs are compatible with an overall decrease of X-ray activity of protostars with time [60].

The absence of matrix in CB_b chondrites indicates a decrease of fine-grained dust with time in the accretion disk. The absence of recycling among CB_b chondrules might be an evidence for the exhaustion of the energy source for making chondrules. CB_b chondrites would thus be the last formed group of chondrites in the solar accretion disk. Such a status might explain some of the bizarreness of CB_b chondrites.

Acknowledgments

We thank Anders Meibom, Sasha Krot, Justin Simon, Eric Feigelson, Jeroen Bouwman, Andreas Pack and Joel Baker for stimulating discussions. Two anonymous reviewers provided comments that helped improve the paper. Caroline Smith (NHM London) and the Meteorite Working Group kindly provided meteorites' sections. Frédéric Couffignal, Omar Boudouma and Rémi Pichon provided valuable help with SEM and EMP. The Programme National de Planétologie and the CNRS France-Etats-Unis program partly funded this project. EDY acknowledges support from the NASA Cosmochemistry program and the NASA Astrobiology Institute. This is IARC publication # 2006-0845.

References

[1] A.N. Krot, Y. Amelin, P. Cassen, A. Meibom, Young chondrules in CB chondrites formed by a giant impact in the early Solar System, Nature 436 (2005) 989–992.

[2] M.K. Weisberg, M. Prinz, R.N. Clayton, T.K. Mayeda, N. Sugiura, S. Zashu, M. Ebihara, A new metal-rich grouplet, Meteorit. Planet. Sci. 36 (2001) 401–418.

[3] A.J. Campbell, M. Humayun, A. Meibom, A.N. Krot, K. Keil, Origin of zoned metal grains in the QUE94411 chondrite, Geochim. Cosmochim. Acta 65 (2001) 163–180.

[4] A.J. Campbell, M. Humayun, M.K. Weisberg, Compositions of unzoned and zoned metal in the CB_b chondrites Hammadah al Hamra 237 and Queen Alexandra Range 94267, Meteorit. Planet. Sci. 40 (2005) 1131–1148.

[5] A. Meibom, M.I. Petaev, A.N. Krot, K. Keil, J.A. Wood, Growth mechanism and additional constraints on FeNi metal condensation in the solar nebula, J. Geophys. Res. 106 (E12) (2000) 32797–32801.

[6] A.N. Krot, A. Meibom, M.I. Petaev, S.S. Russell, J. Aléon, K.D. McKeegan, Y. Amelin, D.C. Hezel, K. Keil, On the origin of chondrules in the CB (Bencubbin-like) carbonaceous chondrite, Geochim. Cosmochim. Acta (submitted for publication).

[7] A.N. Krot, K.D. McKeegan, S.S. Russell, A. Meibom, M.K. Weisberg, J. Zipfel, T.V. Krot, T.J. Fagan, K. Keil, Refractory calcium–aluminum-rich inclusions and aluminum–diopside-rich chondrules in the metal-rich chondrites Hammadah al Hamra 237 and Queen Alexandra Range 94411, Meteorit. Planet. Sci. 36 (2001) 1189–1216.

[8] A. Greshake, A.N. Krot, A. Meibom, M.K. Weisberg, M.E. Zolensky, K. Keil, Heavily-hydrated lithic clasts in CH chondrites and the related, metal-rich chondrites Queen Alexandra Range 94411 and Hammadah al Hamra 237, Meteorit. Planet. Sci. 37 (2002) 281–293.

[9] A. Meibom, K. Righter, N. Chabot, G. Dehn, A. Antignano, T.J. McCoy, A.N. Krot, M.E. Zolensky, M.I. Petaev, K. Keil, Shock melts in QUE 94411, Hammadah al Hamra 237, and Bencubbin: remains of the missing matrix? Meteorit. Planet. Sci. 40 (2005) 1377–1391.

[10] A. Meibom, M.I. Petaev, A.N. Krot, J.A. Wood, K. Keil, Primitive FeNi metal grains in CH carbonaceous chondrites formed by condensation from a gas of solar composition, J. Geophys. Res. 104 (E9) (1999) 22053–22059.

[11] M.A. Ivanova, N.N. Kononkova, I.A. Franchi, A.B. Verchovsky, E.V. Korochantseva, M. Trieloff, A.N. Krot, F. Brandstätter, Isheyevo meteorite: genetic link between CH and CB_b chondrites (abstract), Lunar Planet. Sci. Conf. 37 (2006) 1100.

[12] M.K. Weisberg, M. Prinz, R.N. Clayton, T.K. Mayeda, M.M. Grady, C.T. Pillinger, The CR chondrite clan, Proc. NIPR Symp. Antarct. Meteor. 8 (1995) 11–32.

[13] A.J. Brearley, R.H. Jones, Chondritic meteorites, in: J.J. Papike (Ed.), Planetary Materials, vol. 36, Mineralogical Society of America, Washington D.C, 1998, pp. 3.1–3.398.

[14] A.E. Rubin, G.W. Kallemeyn, J.T. Wasson, R.N. Clayton, T.K. Mayeda, M. Grady, A.B. Verchovsky, O. Eugster, S. Lorenzetti, Formation of metal and silicate globules in Gujba: a new Bencubbin-like meteorite fall, Geochim. Cosmochim. Acta 67 (2003) 3283–3298.

[15] M.I. Petaev, J.A. Wood, A. Meibom, A.N. Krot, K. Keil, The ZONMET thermodynamic and kinetic model of metal condensation, Geochim. Cosmochim. Acta 67 (2003) 1737–1751.

[16] M.I. Petaev, A. Meibom, A.N. Krot, J.A. Wood, K. Keil, The condensation origin of zoned metal grains in Queen Alexandra Range 94411: Implications for the formation of the Bencubbin-like chondrites, Meteorit. Planet. Sci. 36 (2001) 93–106.

[17] A.N. Krot, A. Meibom, S.S. Russell, C.M.O.D. Alexander, T.E. Jeffries, K. Keil, A new astrophysical setting for chondrule formation, Science 291 (2001) 1776–1779.

[18] S.S. Russell, X. Zhu, Y. Guo, N. Belshaw, M. Gounelle, E. Mullane, B. Coles, Copper isotopes in CR, CH-like and CB meteorites: a preliminary study (abstract), Meteorit. Planet. Sci. 38 (2003) A124 (Supp).

[19] J. Zipfel, S. Weyer, Fe-isotopic fractionation in CB chondrites (abstract), Meteorit. Planet. Sci. 41 (2006) 5321 (Supp).

[20] J. Zipfel, S. Weyer, Impact or solar nebula origin of CB chondrites? Evidence from Fe isotopes (abstract), Lunar Planet. Sci. Conf. 37 (2006) 1902.

[21] A. Shukolyukov, G.W. Lugmair, Meteorit. Planet. Sci. 36 (2001) A188–A189 (Supp).

[22] C.M.O'D. Alexander, R.H. Hewins, Mass fractionation of Fe and Ni isotopes in metal in Hammadah al Hamra 237 (abstract), Meteorit. Planet. Sci. 39 (2004) A13 (Supp).

[23] E.D. Young, A. Galy, The isotope geochemistry and cosmochemistry of magnesium, Rev. Mineral. Geochem. 55 (2004) 197–230.

[24] J.I. Simon, E.D. Young, S.S. Russell, E.K. Tonui, K.A. Dyl, C.E. Manning, A short timescale for changing oxygen fugacity in the solar nebula revealed by high-resolution ^{26}Al–^{26}Mg dating of CAI rims, Earth Planet. Sci. Lett. 238 (2005) 272–283.

[25] E.D. Young, J.I. Simon, A. Galy, S.S. Russell, E. Tonui, O. Lovera, Supra-canonical $^{26}Al/^{27}Al$ and the residence time of CAIs in the solar protoplanetary disk, Science 308 (2005) 223–227.

[26] A. Galy, O. Yoffe, P.E. Janney, R.W. Williams, C. Cloquet, O. Alard, L. Halicz, M. Wadhwa, I.D. Hutcheon, E. Ramon,

J. Carignan, Magnesium isotope heterogeneity of isotopic standard SRM980 and new reference materials for magnesium–isotope ratio measurements, J. Anal. At. Spectrom. 18 (2003) 1352–1356.
[27] E.D. Young, A. Galy, H. Nagahara, Kinetic and equilibrium mass-dependent isotopre fractionation laws in nature and their geochemical and cosmochemical significance, Geochim. Cosmochim. Acta 66 (2002) 1095–1104.
[28] E. Stolper, Crystallization sequences of a Ca–Al-rich inclusions from Allende: an experimental study, Geochim. Cosmochim. Acta 46 (1982) 2159–2180.
[29] A. Galy, E.D. Young, R.D. Ash, R.K. O'Nions, The formation of chondrules at high gas pressures in the Solar Nebula, Science 290 (2000) 1751–1753.
[30] M. Bizzarro, J.E. Baker, H. Haack, Mg isotope evidence for contemporaneous formation of chondrules and refractory inclusions, Nature 431 (2004) 275–278.
[31] S.J.K. Symes, D.W.D. Sears, D.G. Akridge, S. Huang, P.H. Benoit, The crystalline lunar spherules: their formation and implications for the origin of meteoritic chondrules, Meteorit. Planet. Sci. 33 (1998) 13–29.
[32] P.H. Warren, E. Tonui, E.D. Young, Magnesium isotopes in lunar rocks and glasses and implcations for the origin of the Moon (abstract), Lunar Planet. Sci. Conf. 36 (2005) 2143.
[33] J.N. Cuzzi, C.M.O'D. Alexander, Chondrule formation in particle-rich nebular regions at least hundreds of kilometers across, Nature 441 (2006) 483–485.
[34] F.M. Richter, A.M. Davis, D.S. Ebel, A. Hashimoto, Elemental and isotopic fractionation of type B calcium-, aluminium-rich inclusions: experiments, theoretical considerations and constraints on their thermal evolution, Geochim. Cosmochim. Acta 66 (2002) 521–540.
[35] R.N. Clayton, R.W. Hinton, A.M. Davis, Isotopic variations in the rock-forming elements in meteorites, Philos. Trans. R. Soc. Lond., A 325 (1988) 438–501.
[36] K. Thrane, M. Bizzarro, J.E. Baker, Brief formation interval for calcium–aluminium-rich inclusions in the early solar system (abstract), Lunar Planet. Sci. Conf. 37 (2006) 1973.
[37] S.B. Simon, L. Grossman, I.D. Hutcheon, R.W. Williams, A. Galy, A.V. Fedkin, R.N. Clayton, T.K. Mayeda, Determination of primordial refractory inclusions compositions (abstract), Lunar Planet. Sci. Conf. 35 (2004) 1684.
[38] S.B. Simon, L. Grossman, A preferred method for the determination of bulk compositions of coarse-grained refractory inclusions and some implications of the results, Geochim. Cosmochim. Acta 68 (2004) 4237–4248.
[39] G.J. MacPherson, A.M. Davis, A petrologic and ion microprobe study of a Vigarano Type B refractory inclusion: evolution by multiple stages of alteration and mixing, Geochim. Cosmochim. Acta 57 (1993) 231–243.
[40] C. Caillet, G.J. MacPherson, E.K. Zinner, Petrologic and Al–Mg isotopic clues to the accretion of two refractory inclusions onto the Leoville parent body: one was hot, the other wasn't, Geochim. Cosmochim. Acta 57 (1993) 4725–4743.
[41] H.W. Weber, E. Zinner, A. Bischoff, Trace element abundances and magnesium, calcium and titanium isotopic compositions of grossite-containing inclusions from the carbonaceous chondrite Acfer 182, Geochim. Cosmochim. Acta 59 (1995) 803–823.
[42] S. Sahjipal, J.N. Goswami, Refractory phases in primitive meteorites devoid of ^{26}Al and ^{41}Ca: representative samples of first solar system solids? Astrophys. J. 509 (1998) L137–L140.
[43] M. Gounelle, F.H. Shu, H. Shang, A.E. Glassgold, K.E. Rehm, T. Lee, The irradiation origin of beryllium radioisotopes and other short-lived radionuclides, Astrophys. J. 640 (2006) 1163–1170.
[44] M. Gounelle, F.H. Shu, H. Shang, A.E. Glassgold, K.E. Rehm, T. Lee, Extinct radioactivities and protosolar cosmic-rays: self-shielding and light elements, Astrophys. J. 548 (2001) 1051–1070.
[45] J.A. Wood, Formation of chondritic refractory inclusions: the astrophysical setting, Geochim. Cosmochim. Acta 68 (2004) 4007–4021.
[46] M. Gounelle, S.S. Russell, Spatial heterogeneity in the accretion disk and early solar chronology, in: A.N. Krot, E.R.D. Scott, B. Reipurth (Eds.), Chondrites and the Protoplanetary Disk, ASP Conference Series, San Francisco, vol. 341, 2005, pp. 548–601.
[47] M. Gounelle, S.S. Russell, On early solar system chronology: implications of an heterogeneous distribution of extinct short-lived radionuclides, Geochim. Cosmochim. Acta 69 (2005) 3129–3144.
[48] S.J. Weidenschilling, Aerodynamics of solid bodies in the solar nebula, Mon. Not. R. Astron. Soc. 180 (1977) 57–70.
[49] J.N. Cuzzi, S.S. Davis, A.R. Doubrovolskis, Blowing in the wind. II. Creation and redistribution of refractory inclusions in a turbulent protoplanetary nebula, Icarus 166 (2003) 385–402.
[50] E.R.D. Scott, S.G. Love, A.N. Krot, Formation of chondrules and chondrites in the protoplanetary nebula, in: R.H. Hewins, R.H. Jones, E.R.D. Scott (Eds.), Chondrules and the Protoplanetary Disk, Cambridge University Press, Cambridge, 1996, pp. 87–96.
[51] J.T. Wasson, G.W. Kallemeyn, Allan Hills 85085: a subchondritic meteorite of mixed nebular and regolithic assemblage, Earth Planet. Sci. Lett. 101 (1990) 148–161.
[52] G.J. MacPherson, D.A. Wark, J.T. Armstrong, Primitive material surviving in chondrites: refractory inclusions, in: J.F. Kerridge, M.S. Matthews (Eds.), Meteorites and Early Solar System, University of Arizona Press, Tucson, 1988, pp. 746–807.
[53] Y. Amelin, A.N. Krot, I.D. Hutcheon, A.A. Ulyanov, Lead isotopic ages of chondrules and calcium–aluminium-rich inclusions, Science 297 (2002) 1678–1683.
[54] E. Zinner, C. Göpel, Aluminum-26 in H4 chondrites: implications for its production and its usefulness as a fine-scaled chronometer for early solar system events, Meteorit. Planet. Sci. 37 (2002) 1001–1013.
[55] K.D. McKeegan, A.M. Davis, Early solar system chronology, in: H.D. Holland, K.K. Turekian (Eds.), Treatise on Geochemistry, Meteorites, Planets, and Comets, vol. 1, Elsevier-Pergamon, Oxford, 2004, pp. 431–460.
[56] A.R. Lyo, W.A. Lawson, E.E. Mamajek, E.D. Feigelson, E.-C. Sung, L.A. Crause, Infrared study of the η Chamaeleontis cluster and the longevity of circumstellar discs, Mon. Not. R. Astron. Soc. 338 (2003) 616–622.
[57] K.E. Haisch, E. Lada, Disk frequencies and lifetimes in young clusters, Astrophys. J. 553 (2001) L153–L156.
[58] L. Hartmann, Astrophysical observations of disk evolution around solar mass stars, in: A.N. Krot, E.R.D. Scott, B. Reipurth (Eds.), Chondrites and the Protoplanetary Disk, ASP Conference Series, vol. 341, 2005, pp. 131–144.
[59] F.H. Shu, H. Shang, T. Lee, Toward an astrophysical theory of chondrites, Science 271 (1996) 1545–1552.
[60] E.D. Feigelson, G.P. Garmire, S.H. Pravdo, Magnetic flaring in the pre-main sequence Sun and implications for the early solar system, Astrophys. J. 584 (2002) 911–930.